THE JOURNAL OF PHYSICAL CHEMISTRY C

Article

pubs.acs.org/JPCC

NMR and X-ray Study Revealing the Rigidity of Zeolitic Imidazolate Frameworks

William Morris,[†] Caitlin J. Stevens,[†,§] R. E. Taylor,*[,†] C. Dybowski,[‡] Omar M. Yaghi,[†,§,∥,⊥] and Miguel A. Garcia-Garibay[†]

[†]Department of Chemistry and Biochemistry, University of California, Los Angeles, Los Angeles, California 90095-1569, United States

[‡]Department of Chemistry and Biochemistry, University of Delaware, Newark, Delaware 19716-2522, United States

[§]Department of Chemistry, University of California, Berkeley, California, 94720, United States

[∥]Molecular Foundry, Division of Materials Sciences, Lawrence Berkeley National Laboratory, Berkeley, California, 94720, United States

[⊥]M. NanoCentury KAIST Institute and Graduate School of EEWS (WCU), Korea

Supporting Information

ABSTRACT: NMR relaxation studies and spectroscopic measurements of zeolitic imidazolate framework-8 (ZIF-8) are reported. The dominant nuclear spin−lattice relaxation (T_1) mechanism for ZIF-8 in air arises from atmospheric paramagnetic molecular oxygen. The ^{13}C T_1 measurements indicate that the oxygen interacts primarily with the imidazolate ring rather than the methyl substituent. Similar relaxation behavior was also observed in a ZIF with an unsubstituted ring, ZIF-4. Single-crystal X-ray diffraction was used to provide data for the study of the thermal ellipsoids of ZIF-8 at variable temperatures from 100 to 298 K, which further confirmed the rigid nature of this ZIF framework. These results highlight a rigid ZIF framework and are in contrast with dynamic metal−organic frameworks based on benzenedicarboxylate linking groups, for which the relaxation reflects the dynamics of the benzenedicarboxylate moiety.

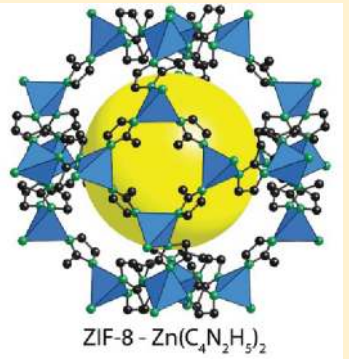

INTRODUCTION

Zeolitic imidazolate frameworks (ZIFs)[1−4] are porous, crystalline frameworks in which the tetrahedral metal ions are linked by imidazolate (Im) units. ZIF structures may be compared with those of zeolites, as the bridging angle formed by this linkage is analogous to that between silicon oxygen and aluminum oxygen units in zeolites. ZIFs are of great interest for numerous applications including gas separation and storage. In contrast with metal−organic frameworks (MOFs),[5] ZIF frameworks have exceptional chemical stability.[1] Highlighting the chemical stability and the importance of ZIF frameworks, ZIF-8 ($Zn(C_4H_5N_2)_2$) is now commercially produced in large quantities by BASF.

The framework mobility of MOFs, particularly the isoreticular metal−organic framework IRMOF series, based on Zn^{2+} with benzenedicarboxylate linkers, has been shown to affect the diffusion of guest molecules within the framework.[6−10] Placing various substituents on the benzenedicarboxylate linkers provides a degree of control of the internal dynamics within MOFs. As specific examples, an activation energy of 11.3 kcal/mol was obtained for the ring-flipping motion for the 1,4-benzenedicarobylate linker.[8] IRMOF-2, containing a bromine substituent on the aromatic ring of the linker, has a rotational barrier of 7.3 kcal/mol.[9] IRMOF-3, with an amino group substituent, lowers the rotational activation energy to only 5.0 kcal/mol.[10] Such efforts may open opportunities for the development of functional materials and artificial molecular machines.[11] In addition to mobility, framework flexibility appears to play a role, as guest molecules have entered framework openings that appear to be smaller than the guest molecules;[12] therefore, an understanding of mobility in ZIFs is essential for accessing the role of diffusion in ZIF frameworks.

The purpose of this work is to investigate the framework mobility in ZIF-8 and ZIF-4 using variable temperature nuclear magnetic resonance spectroscopy and single-crystal diffraction. Previous studies have demonstrated that proton and carbon NMR relaxation in MOFs reflects the local dynamics of the benzenedicarboxylate; however, no studies as of yet have focused on ZIFs. The present experiments demonstrate that in contradistinction to MOF frameworks, NMR relaxation in ZIF-8 has a much different origin and suggests that the linking groups in ZIFs are much more rigid than the linking groups in MOFs.[8−10] Furthermore, substitution of the imidazolate in ZIF-8 does not alter the dynamics of the ring.

Received: April 23, 2012
Revised: May 31, 2012
Published: June 1, 2012

Table 1. Summary of Single-Crystal X-ray Data for ZIFs Collected at Variable Temperature

temperature	100(2) K	200(2) K	240(2) K	298(2) K
empirical formula	$C_{24}H_{30}N_{12}O_3Zn_3$	$C_{24}H_{30}N_{12}O_4Zn_3$	$C_{24}H_{30}N_{12}O_4Zn_3$	$C_{24}H_{30}N_{12}Zn_3$
formula weight	746.7	746.7	746.7	682.4
crystal system	$I\bar{4}3m$	$I\bar{4}3m$	$I\bar{4}3m$	$I\bar{4}3m$
unit cell dimension (Å)	a = 16.8509(3)	16.9122(9)	16.993(2)	17.0095(8)
volume (Å^3)	4784.86(15)	4837.3(4)	4906.8(10)	4921.2(4)
density Mg (m^3)	1.037	1.025	1.011	0.921
crystal size (mm^3)	0.20 × 0.20 × 0.20	0.20 × 0.20 × 0.20	0.20 × 0.20 × 0.20	0.20 × 0.20 × 0.20
reflections collected	11078	10867	8313	10627
independent reflections	573	565	385	500
data/restraints/parameters	573/0/40	565/0/40	385/0/40	500/0/34
goodness of fit on F^2	2.098	1.391	1.393	1.624
final R indices [$I > 2\sigma(I)$]	$R1$ = 0.0688, $wR2$ = 0.2089	$R1$ = 0.0513, $wR2$ = 0.1382	$R1$ = 0.0510, $wR2$ = 0.1424	$R1$ = 0.0477, $wR2$ = 0.1595
R indices all data	$R1$ = 0.0689, $wR2$ = 0.2090	$R1$ = 0.0513, $wR2$ = 0.1382	$R1$ = 0.0512, $wR2$ = 0.1431	$R1$ = 0.0477, $wR2$ = 0.1595

EXPERIMENTAL SECTION

A Bruker Avance 300 spectrometer was used to acquire the NMR data. A standard Bruker ^{1}H wide-line probe with a horizontal 5-mm solenoid radiofrequency (RF) coil was used to acquire proton data for static samples. The sample was confined to the center of the RF coil by two loose plugs of Teflon tape in a 5-mm NMR tube open on both ends. The two open ends allowed the atmosphere of the sample to be switched between air and dry nitrogen gas. The ^{1}H $\pi/2$ pulse width was 1 μs. Proton spin–lattice relaxation (T_1) data were acquired with a saturation-recovery sequence.[13] Using a spin-locking field strength of 62.5 kHz, the ^{1}H spin–lattice relaxation in the rotating frame ($T_{1\rho}$) was determined using a standard spin-locking sequence[13] ($\pi/2_x$ – (spin lock)$_y$).

A magic-angle spinning (MAS) probe with a 4 mm (outside diameter) zirconia rotor was used to acquire high-resolution solid-state ^{13}C and ^{15}N cross-polarization/magic-angle spinning (CP/MAS) data.[14] For the data acquisition, a ^{1}H $\pi/2$ pulse width of 4 μs, a contact time of 5 ms, a data acquisition time of 65 ms, and a recycle delay of at least five times the ^{1}H spin–lattice relaxation time were used. The sample spinning rate was 10.000 (±0.004) kHz. Variable contact time experiments were done using a spin rate of 5.000 (±0.004) kHz.

For a chemical shift scale with tetramethylsilane at zero ppm, the ^{13}C spectra are referenced to the methylene resonance of adamantane at 37.77 ppm as a secondary standard.[15] For ^{15}N spectra referenced to liquid ammonia at zero ppm, the chemical shift was set by use of the ^{15}N resonance of α-glycine at 36.5 ppm as a secondary reference.[16] Nitromethane resonates at 382 ppm on this scale.

Single-crystal X-ray diffraction data for laboratory synthesized ZIF-8 were collected on a Bruker SMART APEXII three-circle diffractometer equipped with a CCD area detector and operated at 1200 W power (40 kV, 30 mA) to generate Cu Kα radiation (λ = 1.5418 Å) at 100(2), 200(2), 240(2), and 298(2) K. The incident X-ray beam was focused and monochromated using Bruker Excalibur Gobel mirror optics. For all cases, frame widths of 0.5° were judged to be appropriate, and full hemispheres of data were collected using the Bruker APEX2[17] software suite to carry out overlapping φ and ω scans at different detector (2θ) settings. Following the data collection, reflections were sampled from all regions of the Ewald sphere to finalize unit cell parameters from the data. Data were integrated using Bruker APEX2 V 2.1 software. Space group determination and tests for merohedral twinning were carried out using XPREP.[18] The highest possible space group was selected ($I\bar{4}3m$), and no evidence of twinning was observed. All variable temperature structures of ZIF-8 were solved using direct methods and were refined with the SHELXTL'97[19] software suite. Final models were refined anisotropically. Crystal-structure and refinement details for ZIF-8 are summarized in Table 1, and CIF files have been deposited in the Cambridge Crystallographic Database (864309–864312). Further structural information at the four temperatures is given in the Supporting Information, Tables S1–S4.

RESULTS AND DISCUSSION

A fragment of the extended structure of ZIF-8 is shown in Figure 1A. ZIF-8 crystallizes in the sodalite (**sod**) topology in the highly symmetric cubic space group $I\bar{4}3m$.[1] Crystal structures have been acquired from data collected at temperatures of 100, 200, 240, and 298 K. Single-crystal diffraction confirms ZIF-8 maintains crystallinity across this temperature range with a small increase in the lattice parameter as the temperature is increased (Table 1), which is consistent with previous neutron diffraction measurements.[20,21] Analysis of thermal ellipsoids was used to evaluate motion in the crystals.[22] Study of the methylimidazolate ring at each temperature offers qualitative insight into the framework flexibility. As shown in Figure 2, the sizes of the thermal ellipsoids of the imidazolate atoms indicate a relatively rigid framework over this temperature range. With the exception of relatively free rotation of the methyl group, no significant increase in size of the thermal ellipsoid is seen across the temperature range. This behavior differs from the mobility of the framework found in MOFs based on Zn^{2+} with benzenedicarboxylate linkers. In addition, from the X-ray diffraction data, a minimum C–C distance between adjacent methyl groups is calculated to be 0.435 nm, making any coupling between the methyl groups very small. Previous neutron diffraction studies at low temperature revealed three-fold rotation of the methyl group was "quasi-free," with a rotational barrier of ~675 J mol^{-1}.[20,21]

NMR spectroscopy is useful in investigating molecular motions across a wide frequency range.[23] The spin–lattice relaxation time, T_1, is sensitive to molecular or group motions on the order of the inverse of the Larmor resonance frequency. The ^{1}H T_1 of a polycrystalline ZIF-8 open to the earth's atmosphere was found to be 0.51 ± 0.07 s at 296 K. Measurement of the ^{1}H T_1 in the same sample flushed with dry nitrogen gas at the same temperature yielded a ^{1}H T_1 of 15.0 ± 0.4 s. The ^{1}H T_1 could be switched between the two extremes

dx.doi.org/10.1021/jp303907p | J. Phys. Chem. C 2012, 116, 13307–13312

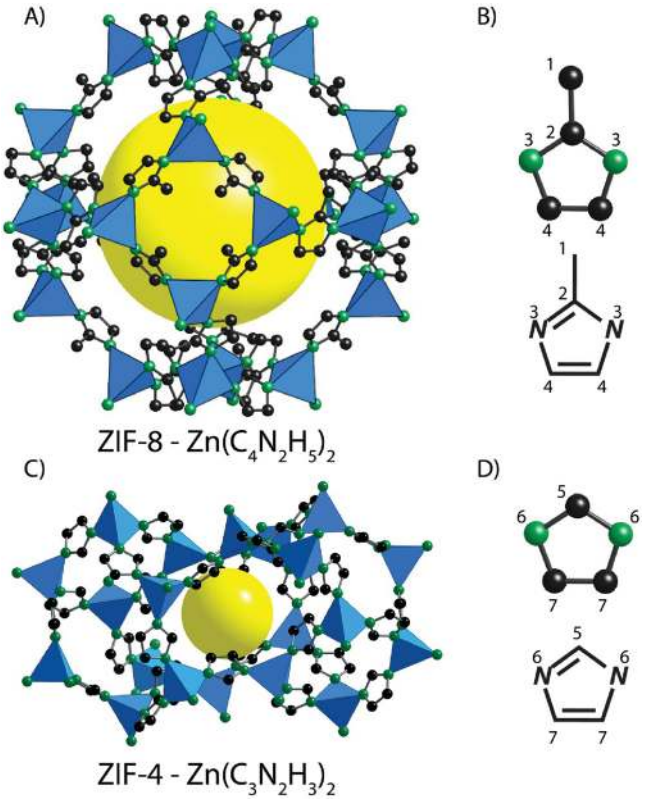

Figure 1. (A) Structure of one **sod** cage of ZIF-8. The yellow sphere represents the free volume within the framework. (B) Assignment of nitrogen and carbon environments in ZIF-8. (C) Structure of one **cag** cage of ZIF-4. The yellow sphere represents the free volume within the framework. (D) Assignment of nitrogen and carbon environments in ZIF-4. Nitrogen (green), carbon (black), and zinc (blue tetrahedra).

by flushing with either air or nitrogen gas after 25 min. Intermediate T_1 values were measured after the switch in gas if the period of purging was less than 25 min.

These measurements suggest that interaction with paramagnetic oxygen is the dominant relaxation mechanism for ZIF-8 exposed to air. Oxygen's effectiveness as a paramagnetic relaxation agent in solution NMR is widely known, and the role of atmospheric oxygen as the dominant source of nuclear spin relaxation has also been shown for solid samples such as silicalites,[24,25] zeolites,[26] and some polymers.[27,28]

To investigate framework motion on the order of the resonance frequency, we performed NMR experiments on the ZIF-8 sample under a nitrogen atmosphere to suppress the paramagnetic relaxation mechanism. Under oxygen-free conditions, the ^{1}H T_1 was found to be relatively constant at 15.0 ± 0.4 s over the temperature range from 230 to 345 K.

For motions on the order of tens of kilohertz, ^{1}H $T_{1\rho}$ values were measured using a spin-locking field of 62.5 kHz, equivalent to that used in the CP/MAS experiments. For hardware reasons, the spin-locking field was not allowed to exceed 30 ms. Little decay of the ^{1}H signal was seen in this temperature range. The ^{1}H $T_{1\rho}$ times obtained from fits to the experimental data were also relatively constant at 150 ± 30 ms. Because no data points could be acquired with spin-locking fields comparable to the relaxation time constant, there is significant uncertainty in the measurements. Nevertheless, the experimentally determined time constants are nearly independent of temperature.

The ^{1}H wide-line NMR spectrum of ZIF-8 is shown in Figure S1 of the Supporting Information. The line is almost featureless, with a width characteristic of broadening due to the effects of dipolar coupling among protons. Very low-frequency motions are typically studied by either spin−spin relaxation (T_2)[13] measurements or by changes in the second moment[29] of the spectra. A classic example is the study of solid benzene,[30] in which the second moment changes by a factor of five with the onset of molecular rotation about the six-fold axis at 100 K. The ^{1}H wide-line spectrum of ZIF-8 does not vary within the temperature range from 230 to 345 K.

The three-fold rotation of the methyl group on the imidazolate is apparently too fast to provide an effective NMR relaxation mechanism over this temperature range. No evidence of slower motions was found.

The ^{13}C CP/MAS spectrum of ZIF-8 in air at 296 K is shown in Figure 3A. Three sharp ^{13}C resonances are observed at 150.5 (2-C), 123.5 (4-C), and 13.3 ppm (1-C, methyl group); the corresponding molecular numbering is given in Figure 1B. The ^{13}C variable−contact−time data for the 4-C resonance at 123.5 ppm, shown in Figure 4, display intense oscillations at multiples of the inverse of the 5 kHz sample rotation speed. These data also show additional less intense oscillations characteristic of the effects of direct dipole−dipole couplings with the protons in strongly coupled solids.[31] No observable shifts in the ^{13}C resonances due to paramagnetic or susceptibility differences were observed when the spectrum was

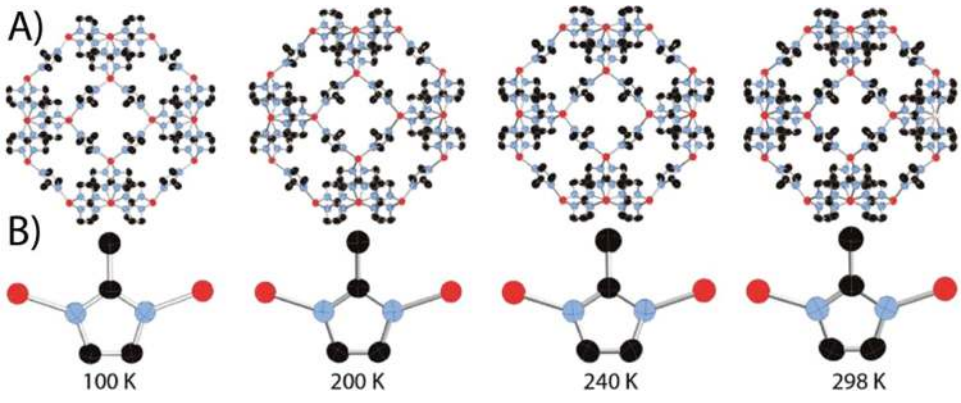

Figure 2. (a) ORTEP representation (50% probability) of **sod** unit of ZIF-8 at 100, 200, 240, and 298 K. (b) ORTEP representation (50% probability) of imidazolate unit of ZIF-8 at 100, 200, 240, and 298 K. Zinc (red), nitrogen (blue), and carbon (black).

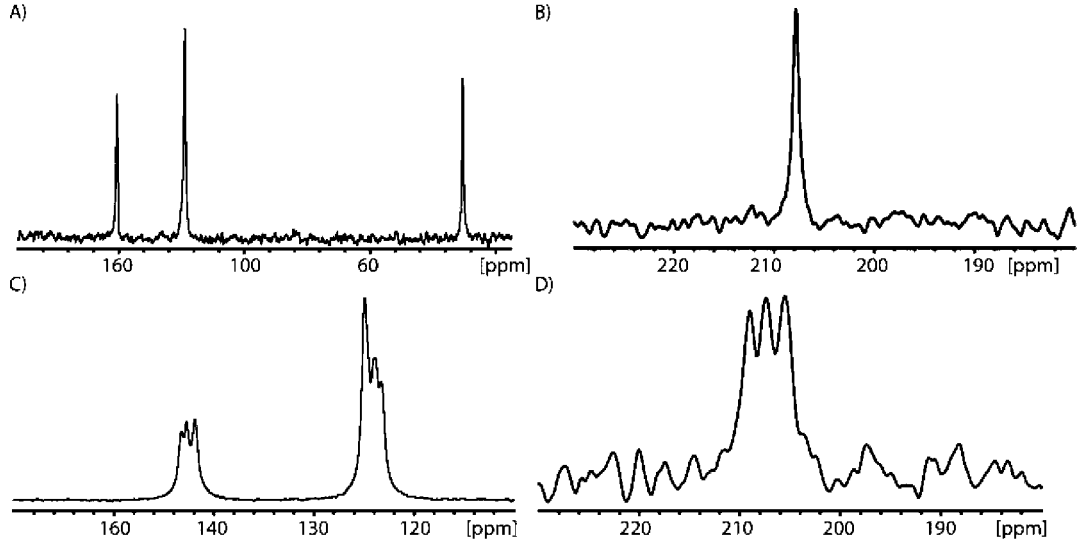

Figure 3. All spectra were obtained in the presence of air. (A) ^{13}C CP/MAS spectrum of ZIF-8 at 296 K. (B) ^{15}N CP/MAS spectrum of ZIF-8 at 296 K. (C) ^{13}C CP/MAS spectrum of ZIF-4 at 296 K. (D) ^{15}N CP/MAS spectrum of ZIF-4 in air at 296 K.

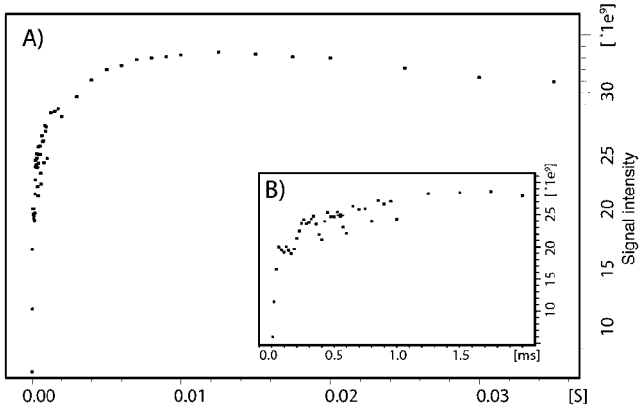

Figure 4. Variable-contact-time ^{13}C CP/MAS data (A) and expansion (B) for the resonance of ZIF-8 in air at 298 K. The nonmonotonic behavior is discussed in the text.

acquired under a nitrogen atmosphere. The ^{13}C variable−contact−time data for the other two resonances are given in the Supporting Information (Figures S1 and S2). As shown in Figure 3B, a single resonance at 208.3 ppm is observed in the ^{15}N CP/MAS spectrum. The ^{15}N variable−contact−time data are shown in Figure S2.

Proton T_1 times can be measured indirectly from the ^{13}C CP/MAS spectrum.[32] The results for this sample are given in Table 2. The T_1 of 0.53 ± 0.03 s obtained by this method is in good agreement with the value 0.51 s obtained by direct observation of the proton resonance. Although the protons are strongly dipolar coupled and hence yield a single-proton relaxation time indicative of the dominant relaxation site, relaxation measurements of the rare ^{13}C spins allow one to probe spatially within the framework. The ^{13}C T_1 relaxation times at the various sites were obtained by Torchia's technique[33] and are reported in Table 2. As previously discussed, the ^1H T_1 is increased in the static sample from 0.5 s in air to 15 s in a nitrogen atmosphere. When the ^1H spin−lattice relaxation time is measured indirectly by ^{13}C NMR combined with MAS for a sample packed in the rotor in air with the rotor driven by compressed air, the same ^1H T_1 of 0.5 s is obtained under MAS. However, when the sample is packed in the rotor under a nitrogen atmosphere with the rotor driven by nitrogen gas, the proton spin−lattice relaxation times become two orders of magnitude longer. It is interesting to note that under the conditions of a nitrogen atmosphere and MAS, the methyl proton T_1 is longer than the T_1 for the other protons. The combination of internal molecular motion, that is, the rotation of the methyl group, and the MAS provides some attenuation of the proton homonuclear coupling, reducing the spin diffusion between the methyl protons and the others.

Table 2. ^1H and ^{13}C NMR Spin−Lattice Relaxation Times for ZIF-8[a]

	carbon resonance position		
sample	150.5 ppm	123.5 ppm	13.3 ppm
ZIF-8 in air			
$^1H^b$	0.50 ± 0.06	0.56 ± 0.06	0.50 ± 0.06
^{13}C	16.6 ± 2	10.4 ± 1.5	6.8 ± 0.7
ZIF-8 in N_2			
$^1H^b$	12.4 ± 1.5	10.9 ± 1.2	14.8 ± 1.6
^{13}C	357 ± 40	702 ± 70	28.4 ± 30

[a]Spin−lattice relaxation times are given in seconds. [b]^1H spin−lattice relaxation times measured indirectly through ^{13}C CP/MAS experiments.

Assuming a dipolar interaction with the paramagnetic oxygen, the rate of relaxation[23] is proportional to $1/(\langle r^6 \rangle)$, where $\langle r^6 \rangle$ is the motionally averaged distance between the nucleus and the oxygen molecule. The effective shortening of the ^{13}C relaxation times of the imidazolate carbons strongly suggests that the molecular oxygen interacts effectively with the imidazolate ring. The relaxation time of the methyl carbon is not lengthened nearly as much in the nitrogen atmosphere as the relaxation times of the other two carbon atoms. This shorter relaxation time of the methyl carbon probably arises from a component of relaxation due to the methyl group rotation. The fact that NMR relaxation suggests that the imidazolate ring appears to be a primary site for gases in ZIF-8 is consistent with a neutron diffraction study that shows the strongest adsorption sites are "directly associated with the organic linkers".[20]

dx.doi.org/10.1021/jp303907p | J. Phys. Chem. C 2012, 116, 13307−13312

Similar NMR relaxation results were obtained for another member of this family, ZIF-4, in which the Zn atoms are linked by an unsubstituted imidazolate. For ZIF-4 in air, paramagnetic oxygen has an even greater effect on nuclear spin relaxation. The ^{1}H T_1 value at 296 K is 63 ± 7 ms, almost an order of magnitude shorter than that measured for ZIF-8. In the presence of nitrogen, the ^{1}H T_1 time increases to 115 000 ± 12 000 ms. The ^{1}H $T_{1\rho}$ time remains relatively long at 60 ± 7 ms for air and nitrogen atmospheres. ZIF-4 crystallizes with a lower symmetry than ZIF-8 in the orthorhombic space group *Pbca*. Unlike ZIF-8 in which all the methylimidazolate rings are equivalent, three individual resonances are resolved in the CP/MAS spectra for each type of carbon atom (Figure 3C) as well as for the nitrogen atom (Figure 3D).

These NMR relaxation results show why ZIFs are so amenable to structural characterization by CP/MAS spectroscopy. The combination of short ^{1}H T_1 and long ^{1}H $T_{1\rho}$ times makes the fast acquisition of high signal-to-noise ^{13}C and ^{15}N spectra possible. Nevertheless, changes in the spin−lattice relaxation times for the framework sites as oxygen is displaced by gases such as CO_2, H_2, and CH_4 may prove to be useful for future investigations using NMR spectroscopy by providing spectral discrimination of the sorbed gases. This work is in contrast with experimental work[12] and theoretical work,[34,35] which showed flexibility under gas pressure. However, the NMR and X-ray experiments described within were performed under the condition of thermal equilibrium and did not expose the framework to changes of gas pressure; therefore, the flexible regimen described by others was not probed.

CONCLUSIONS

In contrast with the mobility of the linker in the IRMOFs, variable-temperature X-ray and NMR experiments show that ZIF-8 has a comparatively rigid framework over the corresponding temperature range of 100 to 298 K. The dominant nuclear spin−lattice relaxation mechanism for ZIF-8 in air arises from interaction of the protons of the imidazolate group with absorbed atmospheric paramagnetic molecular oxygen. The ^{13}C T_1 measurements indicate that the oxygen interacts primarily with the imidazolate ring rather than with the methyl substituent. Similar relaxation behavior is also observed in the unsubstituted ZIF-4. These results contrast the NMR relaxation behavior in the previously investigated IRMOF series. In those cases, local dynamics of the linking groups provide an efficient relaxation mechanism, which allows the determination of dynamic properties such as the activation energy for jumps of the phenyl ring. These results are confirmed by X-ray analysis of ZIF-8 across a wide range of temperatures, which show little change in the size of the thermal ellipsoids across the temperature range, which is indicative of a rigid framework.

ASSOCIATED CONTENT

Supporting Information

Single-crystal X-ray diffraction (SXRD) tables of ZIF-8 and ZIF-4, variable-contact-time ^{13}C CP/MAS analysis of ZIF-8 and ZIF-4. This material is available free of charge via the Internet at http://pubs.acs.org.

AUTHOR INFORMATION

Corresponding Author

*E-mail: taylor@chem.ucla.edu.

Notes

The authors declare no competing financial interest.

ACKNOWLEDGMENTS

This work was supported by National Science Foundation under grant CHE-0956006 (CD), DMR1101934 (MAGG), and as part of the Molecularly Engineered Energy Materials, an Energy Frontier Research Center funded by the U.S. Department of Energy, Office of Science, Office of Basic Energy Sciences under award number DE-SC0001342.

REFERENCES

(1) Park, K. S.; Ni, Z.; Côté, A. P.; Choi, J. Y.; Huang, R.; Uribe-Romo, F. J.; Chae, H. K.; O'Keeffe, M.; Yaghi, O. M. *Proc. Natl. Acad. Sci. U.S.A.* **2006**, *103*, 10186−10191.
(2) Huang, X. C.; Lin, Y. Y.; Zhang, J. P.; Chen, X. M. *Angew. Chem., Int. Ed.* **2006**, *45*, 1557−1559.
(3) Banerjee, R.; Phan, A.; Wang, B.; Knobler, C.; Furukawa, H.; O'Keeffe, M.; Yaghi, O. M. *Science* **2008**, *319*, 939−943.
(4) Phan, A.; Doonan, C. J.; Uribe-Romo, F. J.; Knobler, C. B.; O'Keeffe, M.; Yaghi, O. M. *Acc. Chem. Res.* **2010**, *43*, 58−67.
(5) Rowsell, J. L. C.; Yaghi, O. M. *Microporous Mesoporous Mater.* **2004**, *73*, 3−14.
(6) Amirjalayer, S.; Tafipolsky, M.; Schmid, R. *Angew. Chem., Int. Ed.* **2007**, *46*, 463−466.
(7) Gonzalez, J.; Nandini Devi, R.; Tunstall, D. P.; Cox, P. A.; Wright, P. A. *Microporous Mesoporous Mater.* **2005**, *84*, 97−104.
(8) Gould, S. L.; Tranchemontagne, D.; Yaghi, O. M.; Garcia-Gariby, M. A. *J. Am. Chem. Soc.* **2008**, *130*, 3246−3247.
(9) Winston, E. B.; Lowell, P. J.; Vacek, J.; Chocholoušová, J.; Michl, J.; Price, J. C. *Phys. Chem. Chem. Phys.* **2008**, *10*, 5188−5191.
(10) Morris, W.; Taylor, R. E.; Dybowski, C.; Yaghi, O. M.; Garcia-Garibay, M. A. *J. Mol. Struct.* **2011**, *1004*, 94−101.
(11) Karlen, S. D.; Garcia-Garibay, M. A. *Top. Curr. Chem.* **2005**, *262*, 179−227.
(12) Fairen-Jimenez, D.; Moggach, S. A.; Wharmby, M. T.; Wright, P. A.; Parsons, S.; Düren, T. *J. Am. Chem. Soc.* **2011**, *133*, 8900−8902.
(13) Farrar, T. C.; Becker, E. D. *Pulse and Fourier Transform NMR, Introduction to Theory and Methods*; Academic Press: New York, 1971.
(14) Schaefer, J; Stejskal, E. O. *J. Am. Chem. Soc.* **1976**, *98*, 1031−1032.
(15) Harris, R. K.; Becker, E. D.; Cabal De Menezes, S. M.; Granger, P.; Hoffman, R. E.; Zilm, K. W. *Solid State NMR* **2008**, *33*, 41−56.
(16) Harris, R. K.; Becker, E. D.; Cabal De Menezes, S. M.; Goodfellow, R.; Granger, P. *Pure Appl. Chem.* **2001**, *73*, 1795−1818.
(17) *APEX2*, version 5.053; Bruker AXS, Inc.: Madison, WI, 2005.
(18) *XPREP Software Reference Manual*; Bruker AXS, Inc.: Madison, WI, 2000.
(19) Sheldrick, G. M. *SHELXS'97 and SHELXL'97*; University of Göttingen: Germany, 1997.
(20) Wu, H.; Zhou, W.; Yildirim, T. *J. Am. Chem. Soc.* **2007**, *129*, 5314−5315.
(21) Zhou, W.; Wu, H.; Udovic, T. J.; Rush, J. J.; Yildirim, T. *J. Phys. Chem. A* **2008**, *112*, 12602−12606.
(22) Dunitz, J. D.; Schomaker, V.; Trueblood, K. N. *J. Phys. Chem.* **1988**, *92*, 856−867.
(23) Abragam, A. *Principles of Nuclear Magnetism*; Oxford University Press, Oxford, U.K., 1961.
(24) Cookson, D. J.; Smith, B. E. *J. Magn. Reson.* **1985**, *63*, 217−218.
(25) Li, W.; Lei, X-G; Lem, G.; McDermott, A. E.; Turro, N. J. *Chem. Mater.* **2000**, *12*, 731−737.
(26) Klinowski, J.; Carpenter, T. A.; Thomas, J. M. *J. Chem. Soc., Chem. Commun.* **1986**, 956−958.
(27) Froix, M. F.; Goedde, A. O. *Polymer* **1976**, *17*, 758−760.
(28) Capitani, D.; Segre, A. L.; Blicharski, J. S. *Macromolecules* **1995**, *28*, 1121−1128.
(29) Van Vleck, J. H. *Phys. Rev.* **1948**, *74*, 1168−1183.
(30) Andrew, E. R. *J. Chem. Phys.* **1950**, *18*, 607−618.

(31) Taylor, R. E.; Chim, N.; Dybowski, C. *J. Mol. Struct.* **2007**, *830*, 147−155.
(32) Zumbulyadis, N. *J. Magn. Reson.* **1983**, *53*, 486−494.
(33) Torchia, D. A. *J. Magn. Reson.* **1978**, *30*, 613−618.
(34) Pantatosaki, E.; Megariotis, G.; Pusch, A.-K.; Chmelik, C.; Stallmach, F.; Papadopoulos, G. K. *J. Phys. Chem. C.* **2012**, *116*, 201−207.
(35) Zheng, B.; Sant, M.; Demontis, P.; Suffritti, G. B. *J. Phys. Chem. C.* **2012**, *116*, 933−938.